
Proceedings Paper:
Jahanger, ZK orcid.org/0000-0003-2869-9178 and Antony, SJ orcid.org/0000-0003-1761-6306 (2017) Application of Digital Particle Image Velocimetry in the Analysis of Scale Effects in Granular Soil. In: International Scholarly and Scientific Research & Innovation. ICSMD 2017: 19th International Conference on Soil Mechanics and Dynamics, 17-18 Jul 2017, Rome, Italy. World Academy of Science, Engineering and Technology (WASET) , pp. 910-915.

https://doi.org/10.1999/1307-6892/10007511

Application of Digital Particle Image Velocimetry in the Analysis of Scale Effects in Granular Soil

Zuhair Kadhim Jahanger, S. Joseph Antony

***Abstract*—**The available studies in the literature which dealt with the scale effects of strip footings on different sand packing systematically still remain scarce. In this research, the variation of ultimate bearing capacity and deformation pattern of soil beneath strip footings of different widths under plane-strain condition on the surface of loose, medium-dense and dense sand have been systematically studied using experimental and noninvasive methods for measuring microscopic deformations. The presented analyses are based on model scale compression test analysed using Digital Particle Image Velocimetry (DPIV) technique. Upper bound analysis of the current study shows that the maximum vertical displacement of the sand under the ultimate load increases for an increase in the width of footing, but at a decreasing rate with relative density of sand, whereas the relative vertical displacement in the sand decreases for an increase in the width of the footing. A well agreement is observed between experimental results for different footing widths and relative densities. The experimental analyses have shown that there exists pronounced scale effect for strip surface footing. The bearing capacity factors N_γ rapidly decrease up to footing widths B=0.25 m, 0.35 m and 0.6 m for loose, medium-dense and dense sand respectively, after that there is no significant decrease in N_γ. The deformation modes of the soil as well as the ultimate bearing capacity values have been affected by the footing widths. The obtained results could be used to improve settlement calculation.

***Keywords*—**DPIV, granular mechanics, scale effect, upper bound analysis.

I. Introduction

FOUNDATIONS of building in reality are not very regularly of single size due to design considerations, space limitation, and soil types such as fine soil or granular soil. Cohesionless sand comprises of discrete grains of varying size and packing density. Their mechanical behaviour is different from that of conventional solid, liquid, and gaseous state of matter [1], [2].

In foundation engineering, ultimate bearing capacity and allowable settlement are used as key design parameters [3]. In sand, settlement controls the design of footing [4] which is independent of the loading rate [5]. Also, the settlement of footings could depend on their width for a given soil [5], but ultimate bearing capacity of sand is less dependent on footing width when its width less than 1 m [6]. In soil-structure interaction analysis [7], engineers use constant vertical displacement profile for rigid footings interacting with sand at the level of the footing. However, the displacement in sand could vary significantly below the level of the footing-sand interface within the influence zone of depth about 2-4 times the width of the footing in homogenous sand [8].

Detailed information on how the displacement field evolves within the sand bed under mechanical loading is still not well established. However, experimental results on the role of relative density of sand for all three major types, viz. loose, medium-dense and dense sand as well as the width effects on their geomechanical characteristics are not yet probed systematically. This is addressed here using two-dimensional Digital Particle Image Velocimetry (DPIV). Here, the authors focus on the local deformation and bulk strength for different relative densities of sand when a strip shallow footing of different widths (38 mm, 76 mm and 152 mm) interacts with sand under quasi-static axial loading. Detailed experimental characterisation of the sand material is made using a range of experiments. Finally, using the experimental data, an upper bound theoretical analysis is made to determine the maximum vertical settlement in terms of the ultimate bearing capacity, relative density, and footing width.

The soil deformation pattern and scale effect have received a little or no attention, as most previous studies have chosen materials that represent as nearly as possible the extremes of the foundation, rough (δ/ϕ=1.0) or smooth (δ/ϕ=0). Limited information is available for displacement fields underneath a relatively rough footing in which δ/ϕ=0.25-0.40 under different stress levels.

II. Digital Particle Image Velocimetry

Particle image velocimetry (PIV) is often used in the field of fluid mechanics to track the motion of fluid flow using tracer particles [9]. Recently, PIV has allowed getting a high resolution measurement of soil deformation in geotechnical engineering problems [10], [11]. Dynamic Studio Software Platform (DSSP) is used to analyse the digital images acquired during test using DPIV. This is a suitable method for calculating the velocity vectors of granular flows and their derivatives [12], [13]. This functionality built in the DPIV was used to analyse the digital frames of the grains and to calculate velocity vectors of the grains and their evolution during load application within the sand layer. In this study, the area of interest (full image) was specified before being divided into sub-interrogation areas of 16×16 pixels (mesh of PIV patches), each covering a zone of soil approximately 1.0 mm^2. Each of these patches was tracked using an adaptive PIV method to identify the movement of soil between consecutive images obtained from the front of the

Z. K. Jahanger is a lecturer with Water Resources Engineering Department, College of Engineering, University of Baghdad, Iraq (phone: +964 7901508566, e-mail: zuhairkadhim@yahoo.com). He is now a PhD student at School of Chemical and Process Engineering, University of Leeds, LS2 9JT, Leeds, UK. (e-mail: ml13zkj@leeds.ac.uk).

S. J. Antony is now with School of Chemical and Process Engineering, University of Leeds, LS2 9JT, Leeds, UK (e-mail: S.J.Antony@leeds.ac.uk).

Perspex test rig.

III. Material Properties

The samples used here are disturbed dry silica sand samples obtained in UK. Sand properties were characterised according to the American Society for Testing and Materials [14], [15]. Their experimentally measured material properties and size distribution resulted the following properties: maximum dry density ($\gamma_{dmax.}$) =16.50 kN/m^3 and minimum dry density ($\gamma_{dmin.}$) =14.23 kN/m^3. In addition, using the sieve analysis, the following properties of sand were obtained from the grain size distribution curve: D_{10}=0.25 mm; D_{30}=0.31 mm; D_{60}=0.40 mm (10%, 30%, and 60% of the particles are finer than these particular particle sizes respectively); D_{50}= 0.37 (Mean grain) uniformity coefficient c_u=1.55; and the coefficient of curvature c_c =0.93. The grain shape was mostly spherical, and the angularity of the grains are characterised as angular and sub-angular [15]. These data revealed that the soil chosen is a representative of poorly graded sand [16], [17] which is often encountered in practice.

The peak angle of internal resistance (ϕ_{peak}) for all cases of the packing density was also determined from triaxial compression test at different confining pressures 100, 200, and 300 kPa. For sands, the angle of internal friction typically ranges from 26° to 45°, increasing with the relative density. Three cases of relative densities were used: loose γ=14.65 kN/m^3 D_r=24±2%; medium-dens γ=15.25 kN/m^3, D_r=53± 2%; and dense γ=15.80 kN/m^3, D_r=74 ± 2%. The height of the sand samples was typically 76 mm, and the diameter was about 38 mm. Subsequently, the plots of deviator stress (σ_d) against axial strain (ε_a) were made. The peak angle of friction of the soil is obtained according to the stress state at peak strength. The measured angle of internal friction is 32°, 39°, and 44°. Using these, the peak angle of shearing resistance of the samples was evaluated and plotted against the relative density (D_r). This variation is described in a mathematical form as (1):

$$\phi_{Peak} = 24.7 + 0.267D_r \quad (1)$$

This macroscopic relation is in agreement with the other literature [3]. Two standard penetration tests (CPTs) were also conducted for each soil density and for each footing width to verify the relative density using a 10-mm diameter model CPT [10], [17]. Fig. 1 shows the CPT penetration profiles for the soil for all sand packings. The penetration resistance is plotted against the penetration depth from the bottom level of the footing. The CPTs results for the all densities show the average of the two results (error within 3%).

IV. Experimental Setup and Test Procedure

Bearing capacity tests on footing were conducted in aluminium strong box of 950 mm in length, 650 mm in height, and 39 mm in thickness, filled with sand (Fig. 2). Smooth Perspex front wall of 15 mm thickness is used to eliminate any bending effects.

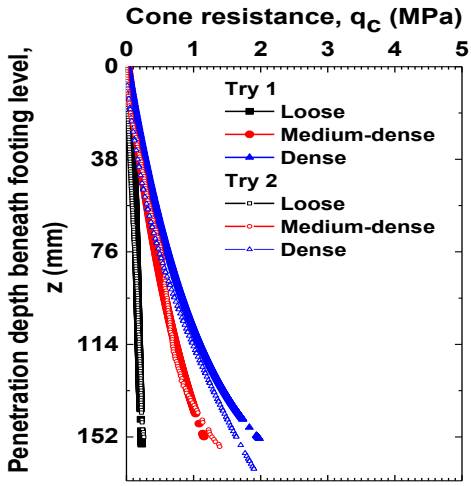

Fig. 1 CPT data for the sand packing

The rigid footings which were located at the sand surface (D_f =depth of footing embedment=0) were relatively rough. The resulting roughness was measured using 3D optical microscopy based on white light interferometry in which the mean roughness value, S_a=3.204 μm (ratio between the angle of interfacial friction of the footing and angle of internal friction of the sand (δ/ϕ) is 0.25). The footing was rigidly connected to the loading machine; therefore, no tilt of the footing was allowed in the experiments. The footings with dimensions of 38 × 38 × 15 mm^3, 76 × 38 × 15 mm^3 and 152 × 38 × 35 mm^3 were used. Footing width B/D_{50} ≥ 100 is adopted to avoid any size effect arising from the relative sizes of the footing and grains and be within the permissible limit [17], [18]. To minimize the scaling effect, it is suggested that the model testing for studying the effect of packing density should not be too close to the density limits, $\gamma_{dmin.}$ and γ_{dmax} [19]. Taking this into account in the present study, the packing densities are kept away from these limits. The model dimension used here is widespread and as used in previous research studies of footing-soil interactions [3], [20]. To minimise any frictional effects of the footing with the wall, a small gap of 1 mm is allowed between the footing and the back wall, so that they do not affect the deformation of the soil recorded by DPIV at the front of the box. These measures ensure that observed movement from images is due to the inner movement in the grains under mechanical loading [21].

The loose granular packing was prepared by pouring the grains uniformly across the width of the box in layers using pouring technique method from Kumar and Bhoi [22] so that any segregation of the grains was avoided during the construction process. The top surface of the sand layer was gently levelled off using a hand scraper. Care was taken not to disturb the constructed loose sample in any way before applying the axial loading in our experiments. The mass of sand grains laid in the box to the required height pertains to the density of the loose sample. The medium-dense packing was achieved in five layers, but using 150 blows per layer by a hand compaction hammer (1000 gm). The dense sand was achieved in seven layers, 200 blows per layer.

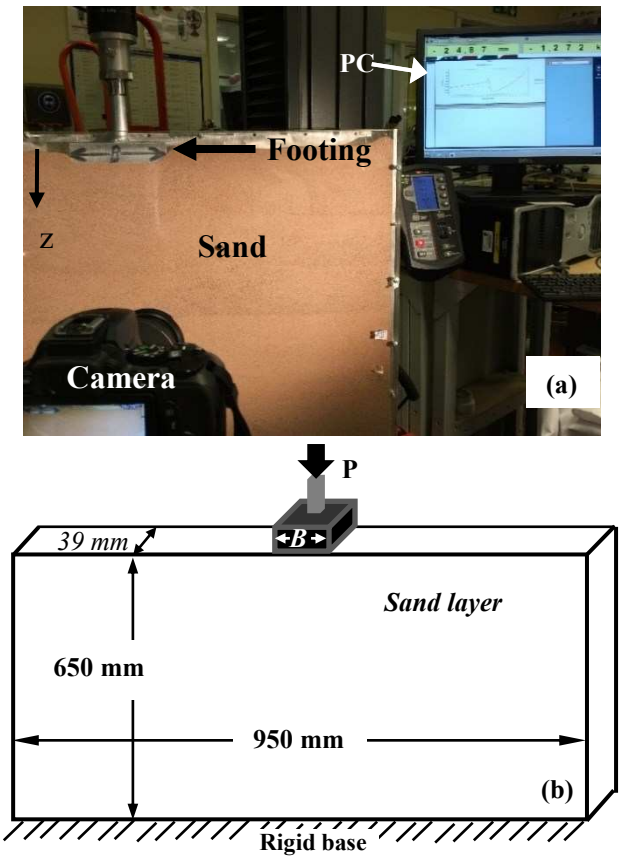

Fig. 2 (a) Experimental setup using DPIV with a live image of single footings in contact (b) definition of the problem, not to scale

An axial compression loading was applied slowly on the footing centre (0.05 mm/s penetration velocity) using Instron loading machine with 250/5.0 kN and 0.1 N resolution (Fig. 2). The macroscopic load and settlement of the footing were also measured from the tests. Nikon D5500 camera that offers high definition (24 Mega Pixels) for more accurate kinematic measurements was fixed in front of the box, and two light sources were used to illuminate the box. However, as the loading condition is quasi-static in this study, an image at every 10 seconds was found to be adequate until the failure of the sand, although higher frame speeds were considered in the early stages of the experimental programme. The resolution of the images was 6000×4000 pixels. DSSP was used to analyse the images using an adaptive DPIV to identify the movement of soil between consecutive images obtained from the front of the Perspex test rig [12], [13]. The distribution of velocity vectors of the grains was examined for which an adaptive interrogation area of size 64 × 64 pixels in 16 × 16 grid step size resolution was employed in the image analysis. In the DPIV analysis, a single grid size was covered by 2-6 grains. The area of interest (full image) was specified before being divided into sub-interrogation areas (mesh of PIV patches), each covering a zone of soil approximately 1.0 mm^2 (16×16 pixels) to a measurement precision of ~ 0.05-0.1 mm/pixel (1 mm =10-20 pixels). The space-pixel dimension of the measurement was calibrated by printing a known scale on the test box along the horizontal and vertical directions. The authors measured the settlement profile from velocity vectors of the granular soil interacting with the footing [23]. Hence, the measurements made here are at the grain-scale (discrete) rather than a continuum measure. The displacement measures (S_R, S_v, and S_h pertaining to the resultant, vertical, and horizontal displacements, respectively) were evaluated under a given load in total (i.e., between the reference image at zero load (q=0) and the image at the required fractions of the ultimate load (q_u) level, such as 0.34q_u and q_u. The results were verified by repeated some tests twice. The difference (error within 5%) was considered to be small, and thus, ignored.

V. Results and Discussions

A. Average Footing Stress versus Settlement

The load–settlement and normalised pressure–strain relationships for all footing widths interacting with sand are shown in Fig. 3. Using the load-settlement data, the tangent intersection method [24] was applied to obtain the value of the ultimate bearing capacity (Fig. 3 (a)). The measured values of the ratio of ultimate vertical settlement (S_u) to footing breadth (B), S_u/B are 3-12%. These ratios increase almost with increasing sand packings, but decrease with footing breadth (Fig. 3 (b)). These measures and the nature of bulk load-settlement curves are consistent [4] with punching (without a well-defined peak), local shear failure (moderate peak) and general shear failure (well-defined peak) for sand described by Vesic [25]. The authors wish to point out that, in the case of strip footings used in practice, 3D condition could exist around the ends of the strip footings even if the footing is long. However, for most parts of long strip footings, plane-strain condition could exist [3], [10], [20] as assumed in the current 2D plane-strain experiments [19]. Though not presented here, we also obtained a very good level of comparison with De Beer's study [26] for the variation of the bearing capacity factor N_γ with γB (density × width) of the footing for different sand packing. The experimental analyses present a rapid decrease in N_γ up to γB=4.0 kPa (or B=0.25 m, 0.35 m and 0.6 m for loose, medium-dense and dense sand respectively), after that there is no significant decrease in N_γ. The bearing pressure increases with the packing density of sand and the footing width as well.

B. Variation of Deformations Components S_v/B and S_h/B with Depth

Previous classical approaches have estimated the elastic settlement of footings using influence factors, which could vary along the depth of sand [3], [27]. Such variations are also observed from numerical solutions, for example using finite element method [27], elastic theory [28], and simple triangular profile using in situ cone penetration tests [8]. However, they show different types of profiles. Using DPIV here, the variation of S_v/B along the centre line of the footing is examined, and S_h/B along the edge of the footing with depth for a typical case of medium-dense sand (B=38 mm) is presented in Fig. 4. They show a nonlinear response for all cases of sand packing. They gradually decrease to a negligible value beyond ~ z/B=3.0, similar results have been reported for loose sand by Liu and

Iskander [16]; however, this distance decreases for an increase in the relative density of sand. The normalised vertical displacement (S_v/B) attains the peak at a depth of about 0.10B for all cases of sand packing and footing widths, which are almost independent of the loading stages.

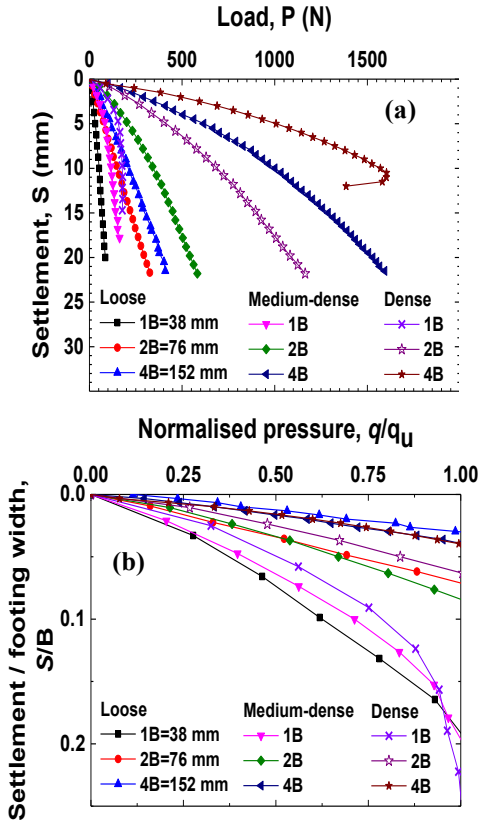

Fig. 3 (a) Load-settlement (b) Normalised pressure-strain curves for different width of footings on loose, medium-dense and dense sand

Similarly, the normalised horizontal displacement (S_h/B) attains maximum at a depth of about 0.25B from the surface of the footing (Fig. 4 (b)). At $q \leq q_u$, the maximum value of normalised vertical displacement for smaller width (B=38mm) is: $S_{v\ max.}/B$ =0.070, 0.086, and 0.096 and $S_{h\ max.}/B$= 0.02, 0.03, and 0.07 for loose, medium-dense, and dense sand, respectively. These values increase with the relative density and load level. But, these values, for the larger width of footing, decrease. Interestingly, the values of $S_{v\ max.}/B$ agree with the common assumption of using S_u/B between 0.05B -0.10B for estimating ultimate bearing capacity q_u from the load-settlement plots in foundation engineering designs [10], [21], [27]. Overall, the displacement measures reported here could be used to derive more realistic description of displacement profiles in soil media in future.

C. Upper Bound Analysis

From the outcomes of the DPIV experiments conducted here, the authors performed an upper bound analysis of the maximum vertical displacements in sand for the footings interacting with different relative densities of sand packing and all widths cases as well. The upper bound analysis does not require to be based on a pre-assumed failure surface profile in the sand. However, it implicitly assumes that, when the rate of work along the failure surface due to external loads is greater or equal to the work done by internal stresses, the external loading cannot exceed the bounds of actual collapse load [29]. Fig. 5 shows the plots of the normalised maximum vertical displacement in the sand for different load levels up to the ultimate load for all footing widths and relative densities. For all cases of the footing width, these measures occurred along the axis of symmetry of the footing.

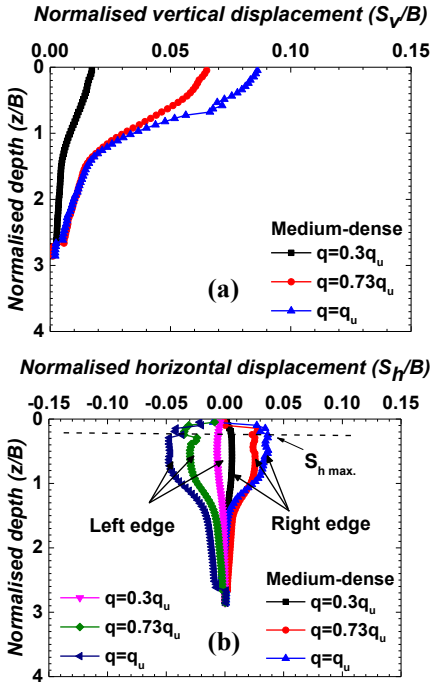

Fig. 4 Settlement profiles with depth z from the bottom surface of the footing at different loading levels: (a) normalised vertical displacement component, (b) normalised horizontal displacement for medium-dense sand packing, B= 38 mm

From these plots, the upper bound curves [30] are drawn as shown in Fig. 5. Large footings were shown to have smaller normalised vertical settlement at ultimate load, which indicates that scale effect exists. The mathematical descriptions of upper bound curves are presented below for the case of footing width 38 mm. Using a functional form $y = x/(a + bx)$, the upper bound lines were drawn as shown in Fig.5, in which $y = q/(q_u)$ and $x = (S_{v\ max.} \times D_r/B)$. For selected values of q/q_u between 0-1, their corresponding values were determined intersecting the upper bound lines (Fig. 5). Substituting these (x and y) values in the above said functional form, the constant a and b were determined. Hence, the final functional form is obtained as:

$$\frac{q}{q_u} = \frac{(S_{v\ max.} \times D_r/B)}{[2.6+0.69\ (S_{v\ max.} \times D_r/B)]}, \quad \text{for } q \leq q_u \qquad (2)$$

Now substituting q/q_u =1.0 in (2), the following equation can be obtained:

$$S_{v\ max.}/B = 8.4/D_r, \quad \text{for B= 38 mm} \qquad (3)$$

The same procedure was followed to derive (4) and (5) pertaining to the maximum vertical displacement in the sand as follows:

$$S_{v\,max.}/B = 6.5/D_r, \text{ for B= 76 mm} \quad (4)$$

$$S_{v\,max.}/B = 3.8/D_r, \text{ for B= 152 mm} \quad (5)$$

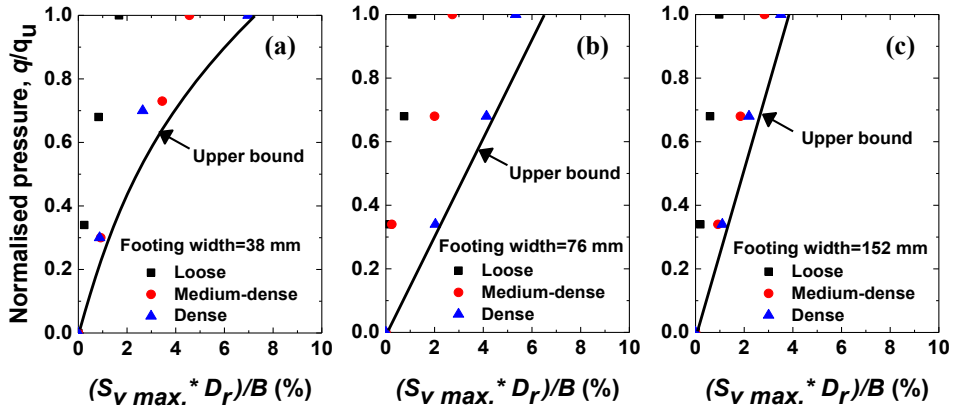

Fig. 5 Normalised ultimate pressure -maximum vertical displacement for different relative densities (a) B=38 mm, (b) B=76mm (c) B=152 mm

D.Variation of Maximum Vertical Displacement with Footing Width and Relative Density Using Upper Bound Analysis

In Fig. 6, the authors present the normalised maximum vertical displacement in the sand under the ultimate load for width of the footings using (3), (4), and (5) respectively for a range of relative density of sand. In this plot, the authors have also superimposed corresponding extrapolated trend for prototype footing. It is evident that, the results from all the approaches are qualitatively similar and quantitatively comparable for relative density great then about 50% (as encountered in most practical conditions).

The DPIV based analysis clearly show that, under the ultimate load level, the normalised vertical displacement ($S_{v\,max.}/B$) in the sand decreases for an increase in the width of the footing (Fig. 6); however, the absolute value of maximum vertical displacement in sand ($S_{v\,max.}$) increases for an increase in the width of the footing [31], [32]. The footing with the largest width produces the smallest $S_{v\,max.}$ under the same relative loading level in agreement with some other conventional studies [30], [33]. Further, this measure decreases rapidly for an increase in the relative density of sand especially up to 70% D_r. For D_r greater than about 90%, the maximum vertical displacement in the soil at ultimate load does not depend on the width of footing in any significant manner. Furthermore, the general trends of this plot are also in agreement with conventional experiments using plate load tests for square and circular plates on granular soil [30], [31], [34]. It is recognised that the scale effects of the footing model could influence the estimations of their strength characteristics as it is related to the critical state line [34]. Cerato and Lutenegger [34] have stated that initial void ratio and stress level to the critical state line affect the footing behavior. For example, a footing with relatively small width would require a relatively low stress level, and hence, it is distant away from the critical state line, as if it was on a denser "state" soil. However, it can be seen that large discrepancies between the measured and the theoretical values were observed in the literature. Therefore, further studies are required to examine this approach for wider strip footing widths.

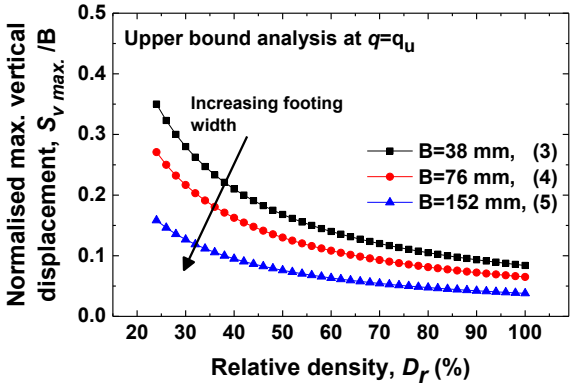

Fig. 6 Variation of normalised maximum vertical displacement in sand under the ultimate load q_u for different cases of footing widths

VI. Conclusion

Investigations into scale effects on soil deformation pattern around strip surface footing of variable widths resting on homogenous granular soil of different relative densities under plain strain condition are carried out. This is addressed here using DPIV. From the results of testing program, the following conclusions may be drawn.

1- The experimental analyses have shown that there exists pronounced scale effect for strip surface footing.
2- The experimental analyses have shown a significant influence of strip surface footing width on vertical deformation of the soil as well as the footing ultimate bearing capacity.
3- The ratios of ultimate vertical settlement of the footing; i.e. the failure settlement (S_u) to footing breadth (B), S_u/B are ~ 3-12%.
4- The upper bound analysis shows that, under the ultimate load level, the normalised vertical displacement ($S_{v\,max.}/B$) in the sand decreases for an increase in the width of the

footing; however, the absolute value of maximum vertical displacement in sand ($S_{v\ max.}$) increases for an increase in the width of the footing.

5- The normalised vertical displacement decreases rapidly for an increase in the relative density of sand especially up to 70% D_r. For D_r greater than about 90%, the maximum vertical displacement in the soil at ultimate load does not depend on the width of footing in any significant manner.

6- The experimental analyses show a rapid decrease in bearing capacity factors $N\gamma$ up to γB=4.0 kPa (or B=0.25 m, 0.35 m and 0.6 m for loose, medium-dense and dense sand respectively) after that there is no significant decrease in $N\gamma$.

REFERENCES

[1] H. M. Jaeger, S. R Nagel, and R. P. Behringer, "Granular solids, liquids, and gases," Rev. *Mod. Phys.*, vol. 68, no.4, pp. 1259-1273, Oct.1996.

[2] S. J. Antony, "Link between single-particle properties and macroscopic properties in particulate assemblies: role of structures within structures," Phil. Trans. R. Soc. A, vol. 365, pp. 2879-2891, Sept. 2007.

[3] J. E. Bowles, *Foundation Analysis and Design*, 5th ed., McGraw-Hill, Singapore, 1997.

[4] B. M. Das, *Shallow foundations: bearing capacity and settlement*, 2nd ed., CRC Press, London, 2009.

[5] C. Liu, and J. B. Evett, *Soils and foundations*, 6th ed., Pearson Prentice Hall, New Jersey, 2004.

[6] K. Terzaghi, and R. B Peck, *Soil mechanics in engineering practice*. Wiley, London, 1967.

[7] S. Hansbo, *Foundation engineering*, Elsevier, London, 1994.

[8] J. H. Schmertmann, P. R. Brown, and J. P. Hartman, "Improved strain influence factor diagrams," *J. Geo. Eng. Div*. vol. 104, no. GT8, pp. 1131-1135, Aug.1978.

[9] R. J. Adrian, "Particle-imaging techniques for experimental fluid mechanics," *Annu. Rev. Fluid Mech.*, vol. 23, pp. 261-304, 1991.

[10] C. O'Loughlin, and B. Lehane, "Nonlinear cone penetration test-based method for predicting footing settlements on sand, "*J. Geo. Geoenviron. Eng.,* vol. 136, no.3, pp. 409-416, Aug. 2010.

[11] T.G. Murthy, E. Gnanamanickam, and S. Chandrasekar, "Deformation field in indentation of a granular ensemble," *Phys. Rev. E*, vol. 85, no.061306, pp.1-11, June 2012.

[12] Z. K. Jahanger, S. J., Antony, J., Richter, "Displacement patterns beneath a rigid beam indenting on layered soil," in Pro. 8th Amer. Reg. Conf. Inter. Soc. Terrain-Vehicle Sys. Michigan, 2016, Paper No.67.

[13] S. Albaraki, and S.J. Antony, "How does internal angle of hoppers affect granular flow? Experimental studies using Digital Particle Image Velocimetry,"*Pow. Techn*., vol. 268, pp. 253-260, Aug. 2014.

[14] ASTM, *American Society for Testing and Materials, Soil and Rock, Building, Stores, Geotextiles*, ASTM Standard, vol. 04.08, 1989.

[15] K. Head, *Manual of Soil Laboratory Test. Volume 1: soil Classification and Compaction Tests*, 3rd ed., CRC Press, Boca Raton, FL, 2006.

[16] J. Liu, and M. Iskander, "Adaptive cross correlation for imaging displacements in soils," *J. Comput. Civil Eng*., vol. 18, no.1, pp. 46-57, Jan. 2004.

[17] J. Dijkstra, D. J. White, and C. Gaudin, "Comparison of failure modes below footings on carbonate and silica sands," *Int. J. Phys. Model. Geotech*., vol. 13, no. 1, pp. 1-12, Aug. 2013.

[18] C.K. Lau, *Scale effects in tests on footings*, PhD thesis, University of Cambridge, UK, 1988.

[19] A. Altaee, and B. H. Fellenius, "Physical modeling in sand," *Can. Geotech. J.* vol. 31, no. 3, pp. 420-431, Feb. 1994.

[20] G.P. Raymond, and F.E. Komos, "Repeated load testing of a model plane strain footing," *Can. Geotech. J.,* vol.15, no. 2, pp. 190-201, Nov. 1978.

[21] D. White, and M. Bolton, "Displacement and strain paths during plane-strain model pile installation in sand," *Géotechnique*, vol. 54, no.6, pp. 375-397, Apr. 2004.

[22] J. Kumar, and M.K Bhoi, "Interference of two closely spaced strip footings on sand using model tests," *J. Geo. Geoenviron. Eng.,* vol. 135, no. 4, pp. 595-604, Apr.2009.

[23] E. Hamm, F. Tapia, and F. Melo, "Dynamics of shear bands in a dense granular material forced by a slowly moving rigid body," *Phys. Rev.* E, vol. 84, no.041304, pp. 1-7, Oct. 2011.

[24] S. O. Akbas, and F. H. Kulhawy, "Axial compression of footings in cohesionless soils. I: Load-settlement behavior," *J. Geotech. Geoenviron. Eng.,* vol.135, no.11. pp. 1562-1574, Nov. 2009.

[25] A.S. Vesic, "Analysis of ultimate loads of shallow foundations," *Soil Mech. and Found. Div., ASCE*, vol.99, no. SM1, pp. 45-73, Jan.1973.

[26] E. E. De Beer, Bearing capacity and settlement of shallow foundations on sand, *in Proc. of Symp. Bearing Capacity and Settlement of Foundation,* Duke University, Durham, N.C. 1965, pp. 15-33.

[27] J. Lee, J. Eun, M. Prezzi, and R. Salgado, "Strain influence diagrams for settlement estimation of both isolated and multiple footings in sand," *J. Geo. Geoenviron. Eng.,* vol.134, no.4, pp. 417-427, Apr. 2008.

[28] P. W. Mayne, and H. G. Poulos, "Approximate displacement influence factors for elastic shallow foundations," *J. Geo. Geoenviron. Eng.,* vol. 125, no. 6, pp. 453-460, June 1999.

[29] W. F. Chen, *Limit Analysis and Soil Plasticity*, J. Ross Publishing, Fort Lauderdale, USA, 2008.

[30] A. J. Lutenegger, and D. J. DeGroot, "Settlement of shallow foundations on granular soils," University of Massachusetts Transportation Center, Amherst, MA 01003, report no. 6332, June 1995.

[31] L. Bjerrum, A. and Eggestad, "Interpretation of loading test on sand." *in Proc. of European Conf. in Soil Mechanics*, Weisbaden, West Germany 1, 1963, pp.199-203.

[32] K. Terzaghi, R. B. Peck, and G., Mesri, *Soil mechanics in engineering practice,* third ed., John Wiley and sons, New York, 1996.

[33] N. F. Ismael, and A. H. N. Ahmad, "Bearing capacity of footings on calcareous sands*." Soils Found*., vol. 30, no. 3, pp.81-90, Sept. 1990.

[34] B. Cerato, and A. J. Lutenegger, "Scale effects of shallow foundation bearing capacity on granular material," *J. Geotech. Geoenviron. Eng*., vol. 133, no. 10, pp.1192-1202, Oct. 2007.